Vol. 40, No. 4 (2018) 670-680, DOI: 10.24874/ti.2018.40.04.13

Tribology in Industry

www.tribology.rs

RESEARCH

Investigation of Cavitation in a Finite Journal Bearing Considering the Journal Speed and Couple Stress Fluids Effects

M.A. Mahdi[a], A.W. Hussain[a] , H.H. Hadwan[a]

[a] *University of Babylon- College of Engineering/ Al-Musayab , Babil, Iraq.*

Keywords:

Journal bearing
Cavitation
Couple stress fluids
Shaft speed

Corresponding author:

Mushrek A. Mahdi
University of Babylon- College of Engineering/ Al-Musayab, Babil, Iraq.
E-mail: engmushrek@yahoo.com

A B S T R A C T

A theoretical analysis of the combined effect of journal speed and couple stress fluids (CSF) on the performance characteristics of a cavitated finite journal bearing (FJB) has been presented in this paper. Depending on the Elrod cavitation algorithm (ECA), the solution to the modified Reynolds equation is achieved. The bearing parameters are affected by both the journal speed and CSF. From the results obtained, it is detected that the non- Newtonian lubricants (CSF) produce enhanced in the fill-film pressure, load-capacity, as well as reduces the Sommerfield number and a small drop in the values of the bearing side leakage flow. The results obtained in this work specify that the characteristics of the bearing are affected significantly by this effect. The achieved results have been compared with that published by other works for the bearing operating with pure lubricant and showed to be in a good agreement.

1. INTRODUCTION

The phenomenon of the cavitation is occurring in several lubricated problems. In tribological environments of a hydrodynamic journal bearing (JB), the lubricant shearing produced high rates of heat, and the rupture in oil film happens in the diverging region of the geometry, where the lubricant film pressure drops below the vapor pressure (vapor cavitation), or below the atmospheric/saturation pressure of the dissolved gases and thus the gas cavities appear. The lubricant properties vary significantly in the cavitated zone. Numerous numerical treatment and relations have been modified to correctly simulate this phenomenon. The Reynolds boundary conditions have been commonly applied due to, it's not complex in applications or employment. Reynolds boundary conditions can't treat the film re-formation boundary and enforce mass-conservation. To treatment the ensure mass continuity and film re-formation, Jakobsson and Floberg [1] and Olsson [2] suggested a model organized known as JFO cavitation model. The JFO model, supposed that the lubricant pressure in the inactive zone is constant ($P = P_{cav}$); therefore, the gradient of the pressure is null in the cavitation (inactive) zone. Also, the model that prepared by JFO offers a set of limits in order to conserve the mass at

the interface between the cavitation and active (full-film) regions at the boundaries of the reformation and rupture. Elrod and Adams [3,4], modified the method of the finite difference that made by the JFO concept, but in a very simple way presented by a single equation for the cavitated and full- film zones. They used an important parameter known as switch function (g) to hold the obtained terms of the pressure within the cavitation zone. The general cavitation algorithm of Elrod-Adams [3,4] remained extremely effective in predictions the performance of the cavitated hydrodynamic JB. Using the switch function, the ECA automatically predicts the conserves mass continuity, cavitation, and full film zones, and calculates the oil film pressure. Vijayaraghavan and Keith [5] developed a cavitation model/algorithm that has used to regulate automatically the finite difference procedure apply to treatment the term of the shear induced-flow and computational efficiency. Dependent on the ECA, a model with a random choice for pressure-density to account for the lubricant bulk modulus (β) variations with pressure has been investigated by Sahlin et al. [6]. They noted that the concluding results are significantly affected by the bulk modulus of the lubricants. Bayada and Chupin [7] and Bayada [8] offered a procedure identical to Elrod-Adams (EA) model through directly solving the constitutive lubricant equations by complete explanations of the mixture characteristics in the non-active zone. They suggested a relationship between the density and pressure like to [8]. Fesanghary and Khonsari [9] presented a new formula for the switch function within the ECA. The classical binary switching function is modified with an exponentially falling or growing function. They concluded that the new switching formulae improve the numerical instability produced by the classical binary switch function. Miraskari et al. [10] suggested a conserving of mass, robust procedure and fast converging for the hydrodynamic pressure of a cavitated JB that has an axial groove dependent on the EA cavitation model. They concluded that the cavitation problem solution strongly depends on the choice values of β.

In conventional hydrodynamic lubrication investigations, Lubricants are supposed to perform as Newtonian lubricants. Several lubrication applications can be found where the pure lubricant constitutive estimate is not a suitable engineering approach to lubrication problems. The performance of the hydrodynamic JB is improved by using a CSF (addition of small quantities of long-chained-polymers additives to a pure lubricant). Due to the existence of these additives, numerous of the lubricants display as the non-Newtonian behavior. Since the standard theory is not valid to describe the rheological behavior of CSF; numerous micro-continuum theories have been made. Among those, the theory of Stokes [11] is a conventional theory in a simple formula which allows for couple stress theory of fluids. Lin [12] studied theoretically the effects of couple stress lubricant on the performance characteristics of FJB and noted that compared with the pure (Newtonian) lubricant, the couple stress lubricant improved the values of the load-capacity and fall the coefficient of the friction. Oliver [13] show that the existence of polymer-additives within the oil or lubricant enhancement the load capacity and reduces the coefficient of friction. Elsharkawy et al. [14] investigated a solution for a hydrodynamics FJB operating with CSF to evaluate the parameter of the couple stress and eccentricity ratio for a known pressure field measured from the experimental test. Wang et al. [15] studied numerically a thermo-hydrodynamic lubrication for FJB operating with CSF dependent on the Stokes couple stress lubricant theory and taking into account the cavitation effect. They used the ECA in the solution of the modified Reynolds equation. Wang et al. [16] analyzed numerically a thermo-hydrodynamic lubrication for a cavitated FJB working with micro-polar lubricants taking into account the effect of the cavitation dependent on the ECA in the solution of the Reynolds equation. The effects of surface roughness and CSF on of the performance of FJB have been studied by Chiang et al. [17]. The effects of the thermal and CSF on the performance of the JB considering cavitation condition have been presented numerically by Kumar et al. [18]. The effects of the turbulence flow (dependent on the turbulent lubrication theory proposed by Constantinescu) and bearing deformable on the static parameters of the hydrodynamic JB operating with non-Newtonian lubricant (CSF) has been studied theoretically by Chetti [19]. According to the results obtained by Chetti, the CSF improves the characteristics of the deformed and non-deformed bearing at the

turbulent and laminar zones. Ayyappa et al. [20] studied theoretically the effects of both the variations of viscosity and roughness of the bearing surface on the performance of the short JB with CSF squeeze film. The performance of the FJB considering the non-Newtonian and bearing elastic deformation effects have been analyzed by Javorova et al. [21].

The purpose of the present paper is to estimate the effects of journal speed and couple stress lubricant on the performance characteristics of a hydrodynamic cavitated FJB. The modified Reynolds equation of isothermal and laminar flow was solved numerically included the cavitation effect (depending on the popular ECA) and couple stress lubricant effect. Also, the difficulties with the abrupt change in the switch function that occur in the numerical solution have been treatment.

2. THE THEORETICAL MODEL FOR CAVITATION PROBLEM

Figure 1 displays the configuration of the journal bearing geometry used in this study. The lubricant pressure field inside the bearing is governed by the Reynolds equation.

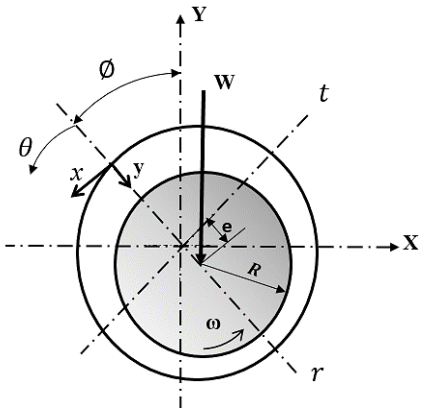

Fig. 1. Journal bearing geometry.

The ECA [5] treatment is considered now as the basic mathematical model. The modified Reynolds equation for isothermal, laminar flow, and under steady-state operating conditions of the hydrodynamic FJB operating with CSF will be developed and is given as [19]:

$$\frac{\partial}{\partial x}\left(\frac{\rho J(h,l)}{\mu}\frac{\partial P}{\partial x}\right)+\frac{\partial}{\partial z}\left(\frac{\rho J(h,l)}{\mu}\frac{\partial P}{\partial z}\right)=6U\frac{\partial \rho h}{\partial x}, \quad (1)$$

Where

$$J(h,l)=h^3-12hl^2+24l^3\tanh\left(\frac{h}{2l}\right). \quad (2)$$

In the cavitation area, the pressure remains constant (i.e., $P=P_{cav}$). The film pressure, density, and the switch function (g) are linked through the bulk modulus of lubricant (β) as [4]:

$$g\beta=\rho\frac{\partial P}{\partial \rho}=\varphi\frac{\partial P}{\partial \varphi}. \quad (3)$$

The above equation can be integrated and gives:

$$P=P_{cav}+g\beta\ln(\varphi), \quad (4)$$

Where φ is the density ratio variable and given as:

$$\varphi=\frac{\rho}{\rho_{cav}} \quad (5)$$

Where P_{cav} and ρ_{cav} Are the lubricant pressure and density in the region of the cavitation. By using the switch function, the terms of the film pressure to be ignored in the inactive zone or to be kept in the active zone. The switch function proposed by [3] is given as:

$$g=\begin{cases}1 & \text{in the active zone} \quad \varphi\geq 1\\ 0 & \text{in the inactive zone} \quad \varphi<1\end{cases}$$

The density ratio φ in the non-cavitation zone is somewhat larger than unity, therefore, Equation (4) can be expressed in a simpler formula [3-5] as:

$$P=P_{cav}+g\beta(\varphi-1). \quad (6)$$

Introducing equations (4) and (5) into the equation (1), the compressible Reynolds equation used in the journal bearing for the new variable φ becomes [15]

$$\frac{\partial}{\partial x}\left(\frac{g\beta J(h,l)}{\mu}\frac{\partial \varphi}{\partial x}\right)+\frac{\partial}{\partial z}\left(\frac{g\beta J(h,l)}{\mu}\frac{\partial \varphi}{\partial z}\right)=6U\frac{\partial}{\partial x}(\varphi h) \quad (7)$$

Where φ has double meanings. φ is the fractional-film content when the lubricant film in the inactive zone while, in the inactive zone, φ is called as the dimensionless density.

To convert the Reynolds equation into the dimensionless form, use the following relations:

$x=R\theta$, $z=\bar{z}L$, $l=\bar{l}c$, $\beta=\frac{\mu_o UR\bar{\beta}}{c^2}$, $\mu=\mu_o\bar{\mu}$, $\bar{h}=h/c=1+\varepsilon\cos\theta$

Then the Reynolds equation in dimensionless formula can be written as:

$$\frac{\partial}{\partial\theta}\left(g\bar{J}(\bar{h},\bar{l})\frac{\partial\varphi}{\partial x}\right)+\left(\frac{R}{L}\right)^2\frac{\partial}{\partial\bar{z}}\left(g\bar{J}(\bar{h},\bar{l})\frac{\partial\varphi}{\partial\bar{z}}\right)= \quad (8)$$

$$6\frac{\bar{\mu}}{\beta}\frac{\partial}{\partial\theta}(\varphi\bar{h}),$$

Where

$$\bar{J}(\bar{h},\bar{l})=\bar{h}^3-12\bar{l}^2\bar{h}+24\bar{l}^3\tanh\left(\frac{\bar{h}}{2\bar{l}}\right). \quad (9)$$

Equation (8) includes numerous special cases. As $\bar{l}=0$, equation (9) reduces to $\bar{J}(\bar{h},\bar{l})=\bar{h}^3$; thus equation (8) converts into the classical Reynolds equation for Newtonian lubricants. Equation (8) can be solved numerically by using a finite difference approach to calculate the φ distributions and then obtained the pressure field from the equation (6).

The boundary conditions of pressure at the bearing edges ($\bar{z}=1$, and $\bar{z}=0$) is given as:

$$\varphi=\exp\left(\frac{\bar{P}_a-\bar{P}_{cav}}{\bar{\beta}}\right). \quad (11)$$

Finally, The oil film pressure distributions are found from the fractional-film content, φ, as:

$$P=\begin{cases}P_{cav}+\beta\ln(\varphi) & \text{if } \varphi\geq 1\\ P_{cav} & \text{if } \varphi<1\end{cases} \quad (12)$$

3. BEARING CHARACTERISTICS

The load capacity of the journal bearing is defined as [19]:

$$W=\sqrt{W_r{}^2+W_t{}^2}\ . \quad (13)$$

Where

$$W_r=\frac{\overline{W}_r\mu LUR^2}{C^2}\int_0^1\int_0^{2\pi}\bar{P}\cos\theta d\theta d\bar{z};$$

$$W_t=\frac{\overline{W}_t\mu LUR^2}{C^2}\int_0^1\int_0^{2\pi}\bar{P}\sin\theta d\theta d\bar{z}\ . \quad (14)$$

And the attitude angle ∅ can be determined from the following equation:

$$\phi=\tan^{-1}\left(-\frac{W_t}{W_r}\right) \quad (15)$$

The bearing side-leakage flow can be obtained from the following equation [19]:

$$Q_s=\frac{UR^2C}{L}\int_0^{2\pi}\frac{\bar{J}(\bar{h},\bar{l})}{12}\left.\frac{\partial\bar{P}}{\partial\bar{z}}\right|_{\bar{z}=0}d\theta\ . \quad (16)$$

The viscous friction force of a shearing film fluids can be expressed as [19]:

$$F_f=\frac{\mu\mathrm{LUR}}{C}\int_0^1\int_0^{2\pi}\left(\frac{1}{\bar{h}}+\frac{\bar{h}}{2}\frac{\partial\bar{P}}{\partial\theta}\right)d\theta d\bar{z}\ . \quad (17)$$

The coefficient of the friction can be calculated by using the relation:

$$C_f=\frac{F_f}{W}(R/C). \quad (18)$$

The Sommerfeld number (S_o) can be found from the relation:

$$So=\frac{\mu\omega LR}{\pi W}\left(\frac{R}{c}\right)^2 \quad (19)$$

4. NUMERICAL PROCEDURE

Hydrodynamic lubrication analysis of a cavitated plain JB considering the effects of couple stress lubricant and shaft (journal) speed required the solution of the Reynolds equation with suitable boundary conditions. This equation is solved numerically by using the finite difference procedure for finding the φ distributions in the domain and then obtained the lubricant pressure distributions.

The main steps of the solution procedure are as follows:

1. Input the operating conditions and lubricant properties, and compute the initial value of attitude angle (∅) is restricted as a first step in the solution procedure, which can be estimated as:

$$\phi=\tan^{-1}\left(\frac{\pi}{4\varepsilon}\left(1-\varepsilon^2\right)^{1/2}\right) \quad (20)$$

2. Assume the initial values of φ and g in the full film region for the first iteration.
3. Compute the new φ distributions by an iterative solution of equation (8) with an under - relaxation factor of (0.95). After each

iteration, g at all points (circumferential and axial) is updated, based on the φ distributions. In some iterations, oscillation and instability are encountered in the solution of Eq. (8) due to the rapid variation in the g at cavitation nodes. For treatment the difficulties with the rapid change in g, used the developed scheme of Fesanghary and Khonsari [9]. Hence, when φ is greater than 1 at any point in the domain, g is increased by dividing the present value by a constant gFactor, $(0 \leq gFactor < 1)$. Otherwise, the value of g is exponentially decreased; in this way, g is replaced by the current value of g times gFactor. The value of g at each point decays to 0 in cavitation zone. The best value of gFactor is 0.8 which is reported in Ref. [9]. The total loop of the iteration is stopped when the convergence criterion of the variable φ reaches (10^{-5}).

4. Compute the oil film pressure from the equation (6).
5. Calculate the load capacity components from the equation (14), then a new value of attitude angle can be calculated from equation (15) and compared with an old angle. The iteration is stopped when the attitude angle convergence criterion reaches (10^{-4}).
6. Calculate the bearing characteristics.

The overall process for the numerical computation is briefly described in the flow chart as shown in Appendix –A

5. RESULTS AND DISCUSSION

The characteristics of a cavitated FJB lubricated by CSF with using different values of the parameter $(\bar{l})$ with the geometric and operating parameters shown in Table 1 have been presented and discussed.

To validate from the numerical method used in the present work, the φ distributions and lubricant pressure of the finite bearing operating with a pure (Newtonian) lubricant that has an eccentricity ratio $\varepsilon = 0.6$ and bulk modules $\bar{\beta} = 40$ has been compared with that calculated by Vijayaraghavan and Keith [5], as presented in Figs. 2 and 3. The above comparison describes a good validation to the Elrod cavitation model as well as the computer code used to solve the governing equation in the current study.

Table 1. Geometric and operating parameters of the journal bearing used in this work.

Bearing Length	$L = 60$ mm
Journal Diameter	$D = 60$ mm
Radial clearance	$C = 145\ \mu m$
Rotational speed	$n = (1000\text{-}4000)$ rpm
Atmospheric pressure	$P_a = 0.0$ pa
Inlet lubricant viscosity	$\mu_o = 0.0277$ pa.s
Cavitation pressure	$P_{cav} = 0.0$ pa
Bulk modulus	$\beta = 6.7 \times 10^9$ pa

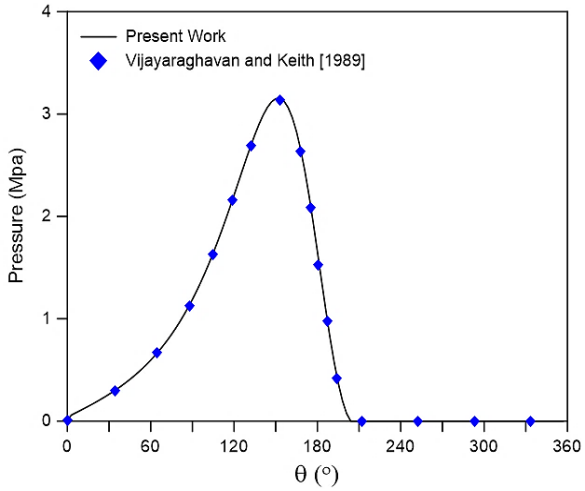

Fig. 2. Comparison between the predicted pressure distributions with that obtained by Vijayaraghavan and Keith [1989] at $\varepsilon = 0.6, \bar{\beta} = 40, L/D = 1.0$.

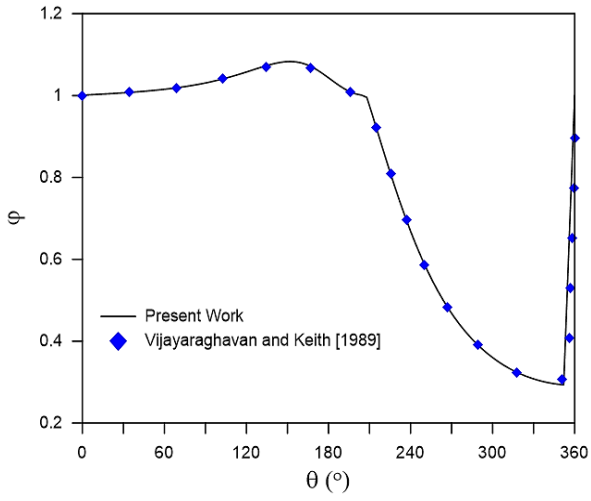

Fig. 3. Comparison between the predicted φ distributions with that obtained by Vijayaraghavan and Keith [1989] at $\varepsilon = 0.6, \bar{\beta} = 40, L/D = 1.0$.

Figure 4 demonstrations the distributions of the lubricant pressure in the active zone with the angular coordinate at the mid-plane of the bearing that operating at $\varepsilon = 0.3$, and 0.6 when using pure

lubricant and couple stress lubricant ($\bar{l} = 0.2$). As clearly shown, the couple stress parameter has a considerable effect on the full-film pressure distribution especially at $\varepsilon = 0.6$. As shown, the film pressure distributions apparently increase with an increase in the values of $\bar{l}$.

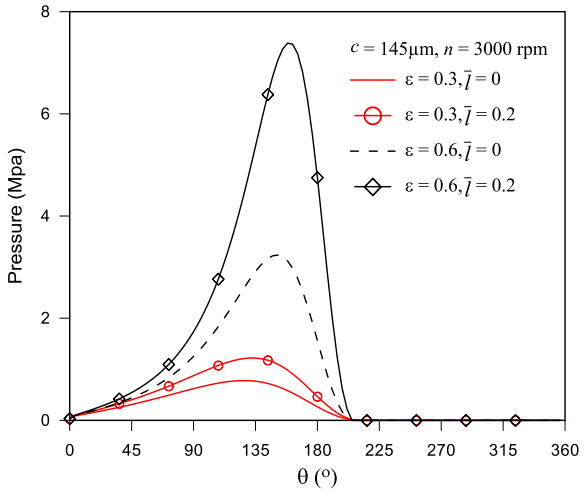

Fig. 4. Effects of both the $\bar{l}$ and ε on the film pressure fields at the mid-plane of bearing $(z = L/2)$.

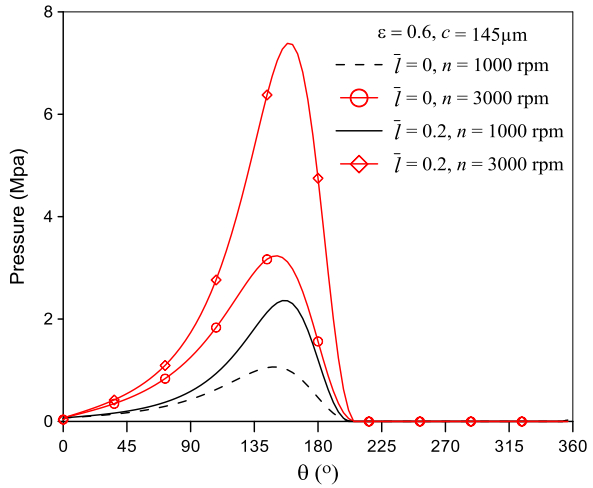

Fig. 5. Effects of both the $\bar{l}$ and n on the film pressure fields at the mid-plane of bearing $(z = L/2)$.

Figure 5 presented the effect of angular shaft speed (n), on the circumferential pressure in active (noncavitated) zone for the finite bearing operating at $\varepsilon = 0.6$ for two lubricant types; Newtonian lubricant and CSF with $(\bar{l} = 0.2)$. It is detected from this figure that the angular speed of the shaft causes an increase in the oil film pressure and this is more noticeable at a higher value of angular speed and when using $(\bar{l} = 0.2)$. The increase in the values of angular speed produces an increase in the values of the dimensionless bulk modules.

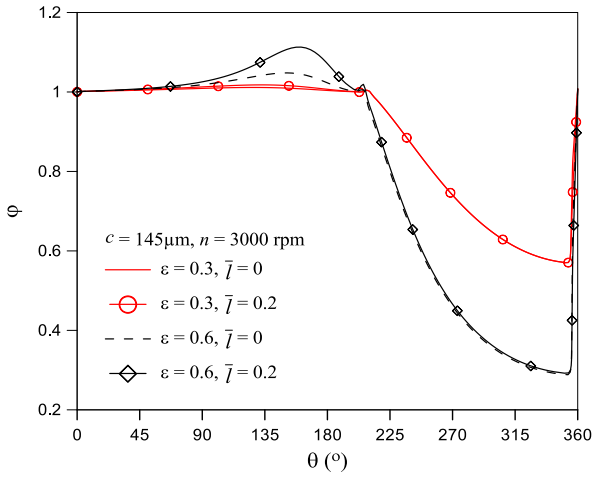

Fig. 6. Effects of both the $\bar{l}$ and ε on the angular distributions of φ.

Figure 6 shows the φ distributions at the mid-plane of the bearing when $\varepsilon = 0.3, 0.6,$ and $n = 3000$ rpm for different values of $\bar{l}$. It is noted that this figure is divided into two regions; the active zone and the inactive region. In the active zone, φ improved with an increase in the values of $\bar{l}$ but, in the inactive zone, the change in values of $\bar{l}$ not effected on the φ distributions. Also, it is obviously shown that when an increase in the value of eccentricity ratio (especially at $\varepsilon = 0.6$, the fractional film content is lower.

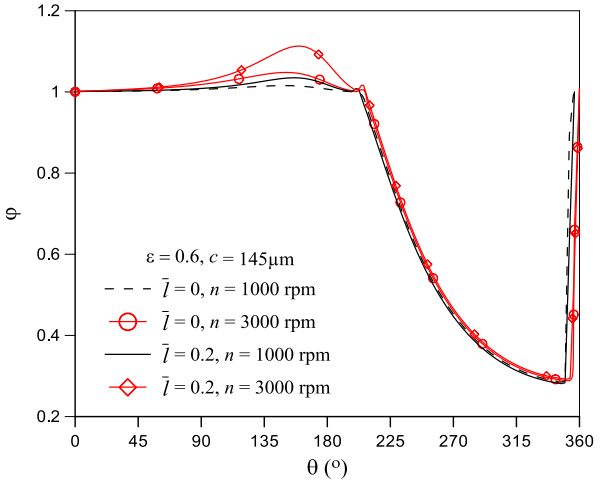

Fig. 7. Effects of both the $\bar{l}$ and n on the angular distributions of φ.

Figure 7 presents the variation of φ with angular coordinates at the mid-plane of the bearing that has $\varepsilon = 0.6$ and when using Newtonian lubricant, and CSF with parameter $\bar{l} = 0.2$. It is detected from this figure that in the active zone, the distributions of φ are improved with the increase in journal speed and this is more obvious when the journal rotating at higher

speed and used couple stress with $\bar{l} = 0.2$. Also, it is detected that, in the inactive zone, the values of φ unchanged with the change in values of shaft speed (n) for both lubricants Newtonian and non-Newtonian, respectively.

The performance parameters of the cavitated journal bearing that have an aspect ratio ($L/D = 1$), rotating shaft speed ($n = 3000$rpm), and radial clearance ($c = 145\ \mu m$), eccentricity ratios ($\varepsilon = 0.2 - 0.8$), and couple stress parameter ($\bar{l} = 0, 0.1, 0.2$) are presented in Figs. 8-15.

Figure 8 displays the variation of the load-capacity with ε for a bearing operating with a lubricant contained polymer additives of different parameter $\bar{l}$. It is shown from this figure that for any value of ε, the behavior of the load-capacity increases with increasing $\bar{l}$. This is due to the enhanced properties of lubricant when added high-long polymer additives to the pure lubricant. Also, it is noted that at higher values of eccentricity ratios the increase in load becomes more obvious, this is due to the rise in oil film pressure.

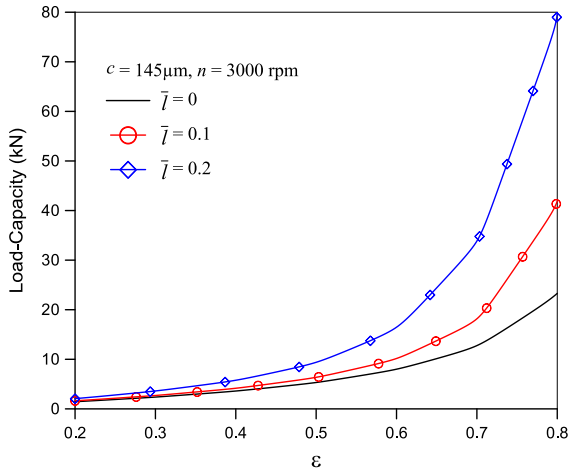

Fig. 8. Load capacity with ε for different $\bar{l}$

Figure 9 demonstrates the variation of load-capacity with journal (shaft) speed for the bearing lubricated with CSF for different values of $\bar{l}$. It is shown from this figure that for any value of speed the CSF parameters ($\bar{l} = 0.1$ and 0.2) produce a noticeable enhancement in the values of the load capacity, and this increase is more clear at higher speeds.

Figure 10 illustrates the bearing side leakage as a function of ε for the cavitated bearing lubricated with CSF. It is clear that the parameter $\bar{l}$ has a little influence on the side leakage. Due to the slight pressure gradient at the bearing ends, the side leakage is slightly decreased with increasing in parameter $\bar{l}$.

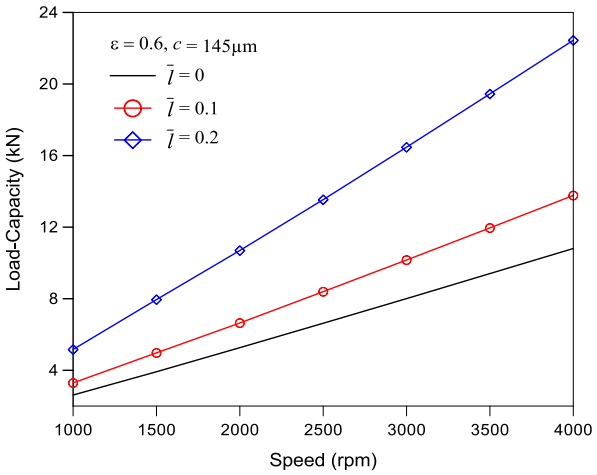

Fig. 9. Load capacity with speed for different $\bar{l}$.

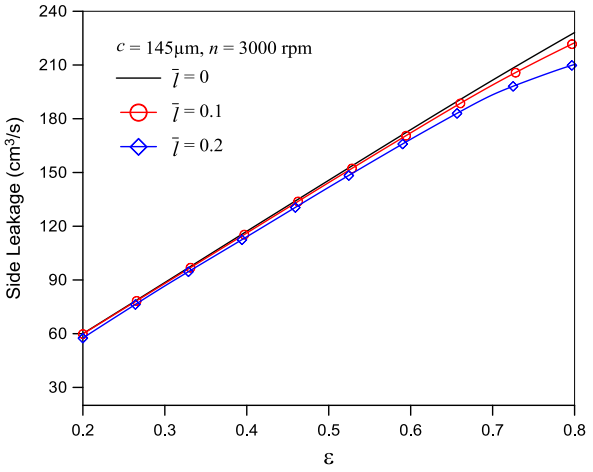

Fig. 10. Side leakage flow with ε for different $\bar{l}$.

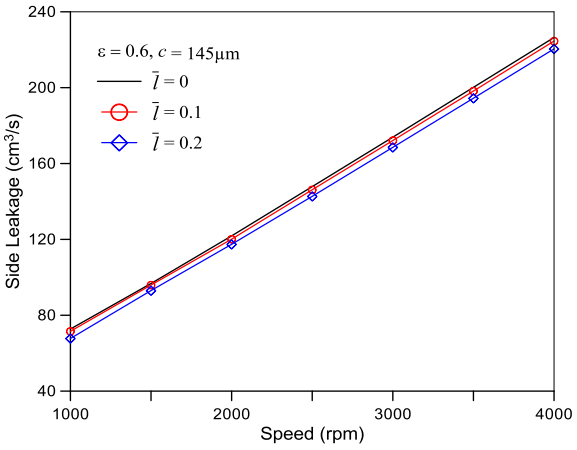

Fig. 11. Side leakage flow with speed for different $\bar{l}$.

Figure 11 exhibits the bearing side leakage flow as a function of shaft speed for different values

of the CSF parameters. From the present figure, it is seen that for any value of the speed, the additional CSF to the pure oil produce an obvious increase in side leakage, especially at higher shaft speeds.

Figures 12 and 13 indicate, respectively, the effect of using polymer additives (CSF) on the decreasing trend of Sommerfeld number and friction coefficient of a finite cavitated bearing. It is clear from these figures that the S_O and C_f reduce when the increase in the CSF parameters, this is because of the growth in bearing load carrying capacity. These figures clearly show that the S_O and C_f are significantly affected when the bearing lubricated with the higher value of $\bar{l}$.

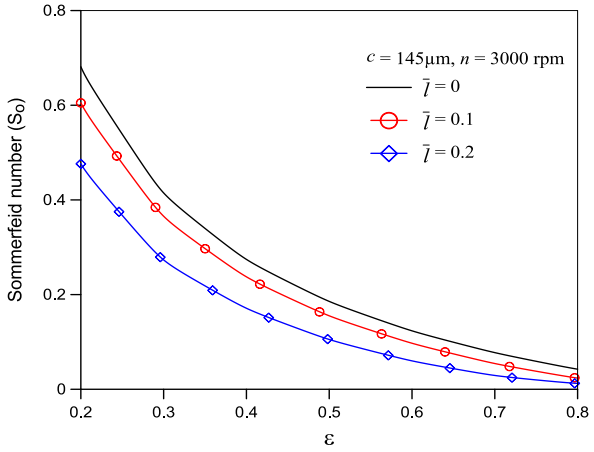

Fig. 12. Sommerfeld number with ε for different $\bar{l}$.

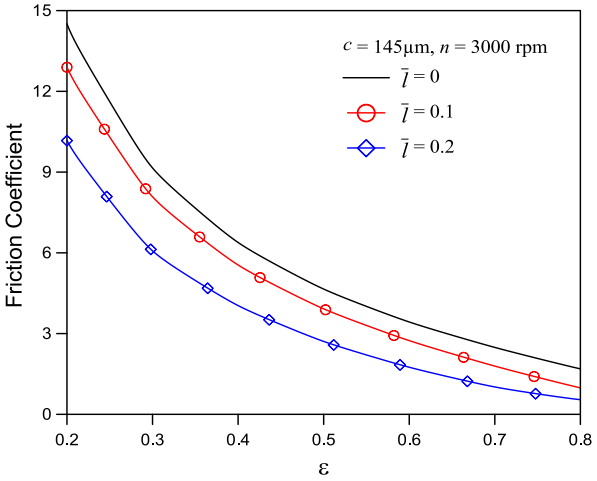

Fig. 13. Friction coefficient with ε for different $\bar{l}$.

Figures 14 and 15 show, respectively, the variation of the S_O and C_f with journal angular speed for different values of $\bar{l}$. It is seen that for any value of speed the CSF yield decreased in both the S_O and C_f.

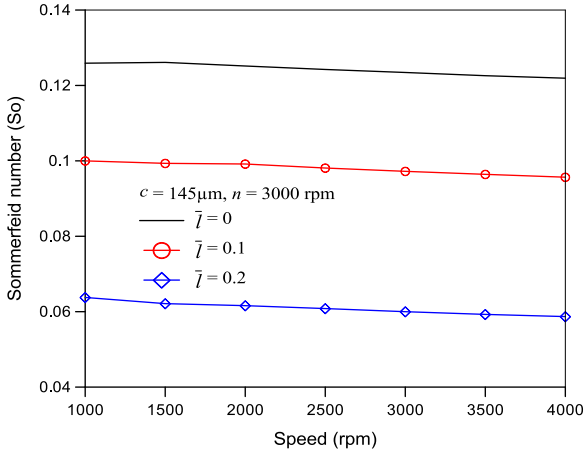

Fig. 14. Sommerfeld number with speed for different $\bar{l}$.

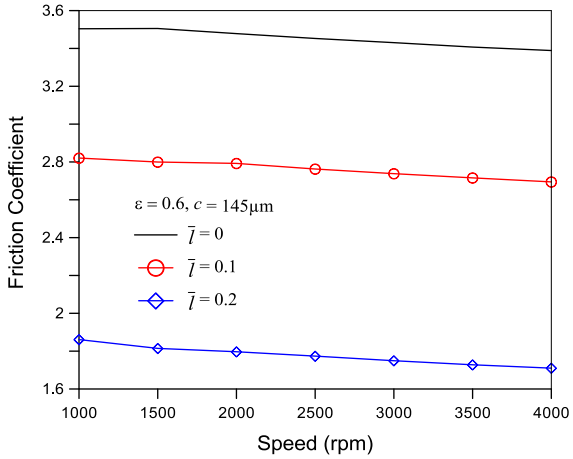

Fig. 15. Friction coefficient with speed for different $\bar{l}$.

The contours of φ for both Newtonian and CSF ($\bar{l} = 0.3$) when the journal operating with $n = 3000$ rpm and $\varepsilon = 0.6$ have been offered in Fig. 16. From this figure, it is detected that contours divided into two regions, one is the convergent (non-cavitation) zone and the second is the divergent (cavitation) zone.

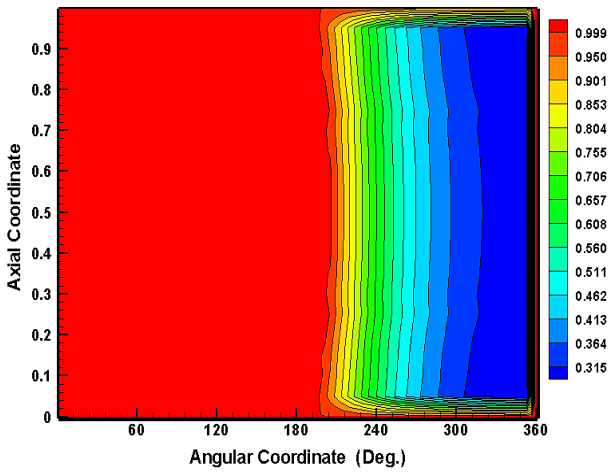

(a) $\bar{l} = 0$

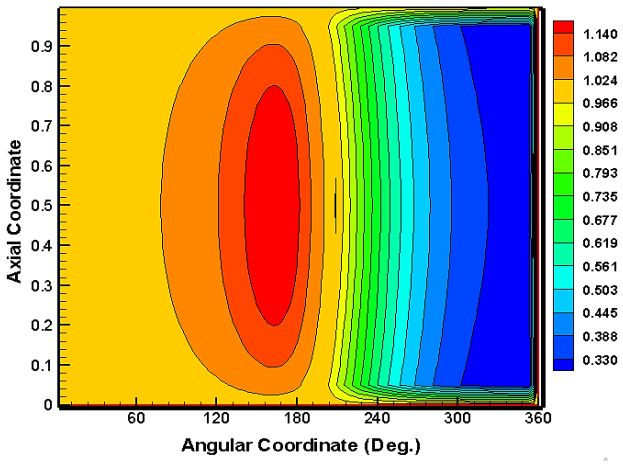

(b) $\bar{l} = 0.3$

Fig. 16. Effects of $\bar{l}$ on the φ contours for the case, $\varepsilon = 0.6, n = 3000$ rpm.

Also, it is seen that when the increase in the parameter $\bar{l}$, the values of φ contours in the non-cavitation zone are growth while, in the cavitation zone, the change in values of $\bar{l}$ not effected on the values of φ contours.

6. CONCLUSION

1. The couple stress parameter $\bar{l}$ has a considerable effect on the full-film pressure especially at $\varepsilon = 0.6$. The pressures obviously increase with increase in $\bar{l}$.
2. The pressure in the non-cavitation zone increase with the increase in speed of the shaft this is more clear at a higher value of the speed and when using the higher value of $\bar{l}$.
3. In the full-film zone, φ (dimensionless density) is improved with the increase in $\bar{l}$ and speed n this is more obvious at higher speed and when used $\bar{l} = 0.2$ while, in the cavitated zone, φ (fractional film content) remain constant with increase in $\bar{l}$ and n.
4. In the cavitated region, when an increase in the value of ε, the φ (fractional-film-content) is lower.
5. The load capacity, improved by increasing the speed and $\bar{l}$ while the side leakage and Sommerfeld number decreased with increasing the speed and $\bar{l}$.

REFERENCES

[1] B. Jakobsson, L. Floberg, *The Finite Journal Bearing Considering Vaporization*, Göteborg, Gumperts Förlag, Sweden, 1957.

[2] K.-O. Olsson, *Cavitation in Dynamically Loaded Bearing*, Göteborg: Akademiiörlaget, Gumperts, 1965, Sweden, 1965.

[3] H. Elrod, M. Adams, *A Computer Program for Cavitation and Starvation Problems, Cavitation and Related Phenomena in Lubrication*, Mechanical Engineering Publications, New York, 1974.

[4] H.G. Elrod, *A Cavitation Algorithm*, ASME Journal of Tribology, vol. 103, iss. 3, pp. 350–354, 1981, doi:10.1115/1.3251669

[5] D. Vijayaraghavan, T.G. Keith, *Development and Evaluation of a Cavitation Algorithm*, Tribology Transactions, vol. 32, iss. 2, pp. 225–233, 1989, doi: 10.1080/10402008908981882

[6] F. Sahlin, A. Almqvist, R. Larsson, S. Glavatskih, *A Cavitation Algorithm for Arbitrary Lubricant Compressibility*, Tribology International, vol. 40, iss. 8, pp. 1294–1300, 2007, doi: 10.1016/j.triboint.2007.02.009

[7] G. Bayada, L. Chupin, *Compressible Fluid Model for Hydrodynamic Lubrication Cavitation*, ASME Journal of Tribology, vol. 135, iss. 4, pp. 041702-1 to 041702-13, 2013, doi: 10.1115/1.4024298

[8] G. Bayada, *From a Compressible Fluid Model to New Mass Conserving Cavitation Algorithms*, Tribology International, vol. 71, pp. 38–49, 2014, doi: 10.1016/j.triboint.2013.10.014

[9] M. Fesanghary, M. M. Khonsari, *A Modification of the Switch Function in the Elrod Cavitation Algorithm,* ASME Journal of Tribology, vol. 133, iss. 2, pp. 024501-1 to 024501-4, 2011, doi: 10.1115/1.4003484

[10] M. Miraskari, F. Hemmati, A. Jalali, M.Y. Alqaradawi, *A Robust Modification to the Universal Cavitation Algorithm in Journal Bearings*, ASME Journal of Tribology, vol. 139, iss. 3, pp. 031703-1 to 031703-17, 2016, doi: 10.1115/1.4034244

[11] V.K. Stokes, *Couple stresses in fluids*, Physics of Fluids, vol. 9, pp. 1709–1715, 1966, doi: 10.1063/1.1761925

[12] L.R. Lin, *Effects of couple stresses on the lubrication of finite journal bearings*, Wear, vol. 206, iss. 1&2, pp. 171–178, 1997, doi: 10.1016/S0043-1648(96)07357-7

[13] D.R. Oliver, *Load enhancement effects due to polymer thickening in a short model journal bearing*, Journal of Non-Newtonian Fluid

Mechanics, vol. 30, iss. 2&3, pp. 185-196, 1988, doi:10.1016/0377-0257(88)85024-9

[14] A.A. Elsharkawy, L.H. Guedouar, *An inverse solution for finite bearings lubricated with couple stress fluids*, Tribology International, vol. 34, iss. 2, pp. 107–118, 2001, doi: 10.1016/S0301-679X(00)00145-6

[15] X.L. Wang, K.Q. Zhu, S.Z. Wen, *A study of a journal bearing lubricated by couple stress fluids considering thermal and cavitation effects*, Institution of Mechanical Engineers, Part J: Journal of Engineering Tribology, vol. 216, iss. 5, pp. 293-305, 2002, doi: 10.1243/135065002760364831

[16] X.L. Wang, K.Q. Zhu, *Numerical Analysis of Journal Bearing with Micropolar Fluids Including Thermal and Cavitating Effects*, Tribology International, vol. 39, iss. 3, pp. 227–237, 2006, doi: 10.1016/j.triboint.2005.01.028

[17] H.L. Chiang, C.H. Hsu, J.R. Lin, *Lubrication Performance of Finite Journal Bearings Considering Effects of Couple Stresses and Surface Roughness*, Tribology International, vol. 37, iss. 4, pp. 297 307, 2004, doi: 10.1016/j.triboint.2003.10.005

[18] V.B. Kumar, P. Suneetha, K.R. Prasad, *Lubrication of Journal Bearing Considering Thermal Effect in Couple Stress Fluid Considering Cavitation*, International Journal of Advanced Research, vol. 1, iss. 2, pp. 59 – 66, 2013.

[19] B. Chetti, *Combined effects of turbulence and elastic deformation on the performance of a journal bearing lubricated with a couple stress fluid*, Institution of Mechanical Engineers, Part J: Journal of Engineering Tribology, pp. 1-7, 2018. doi: 10.1177/1350650118757555

[20] G.H. Ayyappa, N.B. Naduvinamani, A. Siddangoudac, S.N. Biradar, *Effects of Viscosity Variation and Surface Roughness on the Couple Stress Squeeze Film Characteristics of Short Journal Bearings*, Tribology in industry, vol. 37, no. 1, pp. 117-127, 2015.

[21] J. Javorovaa, A. Mazdrakovaa, I. Andonovb, A. Radulescu, *Analysis of HD Journal Bearings Considering Elastic Deformation and Non-Newtonian Rabinowitsch Fluid Model,* Tribology in industry, vol. 38, no. 2, pp. 186-196, 2016.

NOMENCLATURE

c	: Radial clearance (m)
C_f	: Friction coefficient
e	: Eccentricity (m)
F_f	: Viscous friction force (N)
g	: Switch function
h	: Film thickness (m)
$\bar{h}$	: Non-dimensional lubricant film thickness, $\bar{h} = h/c$
L	: Length of the bearing (m)
l	: characteristic additives length, (m) $l = \sqrt{\eta/\mu}$
$\bar{l}$	: parameter of the couple stress lubricant, $\bar{l} = l/C$
n	: Rotational speed (rpm)
P	: Hydrodynamic oil film pressure (pa)
P_a	: Ambient pressure (Pa)
P_{cav}	: Cavitation pressure (Pa)
Q_S	: Leakage flow rate (m^3/s)
R	: Radius of journal (m)
S_O	: Sommerfeld number
W	: Total load capacity (N)
W_r, W_t	: Radial and tangential load capacity components, respectively (N)
U	: Journal linear speed ($U = \omega R$), (m/s)
x, z	: Coordinates system (m)
$\bar{z}$	: Dimensionaless axial coordinates respectively
φ	: Fractional film content in the inactive zone; non-dimension density in the active zone
β	: Oil bulk modulus (Pa)
ε	: Eccentricity ratio, $\varepsilon = e/C$
η	: Material constant to blame for the CSF property
θ	: Circumferential coordinate, x/R, (degree)
μ	: Viscosity of the lubricant (pa. s)
ρ	: Lubricant density (kg/m^3)
$\emptyset$	: Attitude angle (degree)
ω	: Angular velocity of the shaft, (rad/s)

Appendix A. Flow chart of numerical computation.